HHS Public Access

Author manuscript

Brain Res. Author manuscript; available in PMC 2018 April 01.

Published in final edited form as:

Brain Res. 2017 April 01; 1660: 36–46. doi:10.1016/j.brainres.2017.02.001.

Brain network alterations in the inflammatory soup animal model of migraine

Lino Becerra[1,2,3], **James Bishop**[1,2], **Gabi Barmettler**[1,2], **Vanessa Kainz**[4,†], **Rami Burstein**[4,**,†], and **David Borsook**[1,2,3]

[1]Pain/Analgesia Imaging Neuroscience (P.A.I.N.) Group, Department of Anesthesia, Boston Children's Hospital, Center for Pain and the Brain, Harvard Medical School, Boston, MA, USA

[2]Athinoula A. Martinos Center for Biomedical Imaging, Massachusetts General Hospital, Charlestown, MA, USA

[3]Departments of Psychiatry and Radiology, Massachusetts General Hospital, Harvard Medical School, Charlestown, MA 02129, USA

[4]Department of Anaesthesia and Critical Care, Beth Israel Deaconess Medical Center, Harvard Medical School, Boston, MA 02215, USA

Abstract

Advances in our understanding of the human pain experience have shifted much of the focus of pain research from the periphery to the brain. Current hypotheses suggest that the progression of migraine depends on abnormal functioning of neurons in multiple brain regions. Accordingly, we sought to capture functional brain changes induced by the application of an inflammatory cocktail known as inflammatory soup (IS), to the dura mater across multiple brain networks. Specifically, we aimed to determine whether IS alters additional neural networks indirectly related to the primary nociceptive pathways via the spinal cord to the thalamus and cortex. IS comprises an acidic combination of bradykinin, serotonin, histamine and prostaglandin PGE2 and was introduced to basic pain research as a tool to activate and sensitize peripheral nociceptors when studying pathological pain conditions associated with allodynia and hyperalgesia. Using this model of intracranial pain, we found that dural application of IS in awake, fully conscious, rats enhanced thalamic, hypothalamic, hippocampal and somatosensory cortex responses to mechanical stimulation of the face (compared to sham synthetic interstitial fluid administration). Furthermore, resting state MRI data revealed altered functional connectivity in a number of networks previously identified in clinical chronic pain populations. These included the default mode, sensorimotor, interoceptive (Salience) and autonomic networks. The findings suggest that activation and sensitization of meningeal nociceptors by IS can enhance the extent to which the

Corresponding Author: Lino Becerra PhD, Pain/Analgesia Imaging Neuroscience (P.A.I.N.) Group, Department of Anesthesia, Boston Children's Hospital, Boston, MA 02215, USA, Tel: 781 216 1199, lino.becerra@childrens.harvard.edu.

†Co-Last Authors

The authors declare no competing financial interests.

brain processes nociceptive signaling, define new level of modulation of affective and cognitive responses to pain; set new tone for hypothalamic regulation of autonomic outflow to the cranium; and change cerebellar functions.

Keywords

fMRI; rat; migraine; inflammatory soup; resting state networks

1. Introduction

Current hypotheses suggest that the progression of migraine depends on abnormal functioning of neurons in multiple brain regions (Bahra et al., 2001; Burstein et al., 1998b; Burstein et al., 2000b; Burstein et al., 2010; Coppola and Schoenen, 2012). Magnetic resonance imaging (MRI) has been used extensively to investigate changes in brain structure and function in clinical populations of migraine including resting state functional connectivity differences (Liu et al., 2015; Russo et al., 2012; Yuan et al., 2013). Capitalizing on mounting clinical evidence to support brain alterations by pain, and more specifically migraine, there is a critical need to improve the reliability of pre-clinical animal models for basic pain research. Though many animal models of migraine exist (Romero-Reyes and Akerman, 2014; Storer et al., 2015) the validity of these models to recapitulate clinical brain pathophysiology is often ambiguous. Here we focus on a promising rat model of migraine known as the inflammatory soup (IS) model utilizing an fMRI neuroimaging approach to investigate the alterations in brain response to mechanical and thermal stimulation as well as resting state functional connectivity.

Inflammatory soup (IS) is an acidic combination of a mixture of bradykinin, serotonin, histamine and prostaglandin PGE2. It was conceptualized based on analyzed samples of inflamed human tissues (Steen et al., 1995), introduced to basic pain research as a tool to activate and sensitize peripheral nociceptors (Steen et al., 1992; Steen et al., 1996), and used extensively to induce animal models of pathological pain conditions associated with allodynia and hyperalgesia (De Felice et al., 2013; Oshinsky and Gomonchareonsiri, 2007). For example, IS has been shown to be efficacious at inducing sensitization upon administration to sensory fibers innervating a host of anatomical structures including: cutaneous tissue and nerve fibers (Katz and Gold, 2006; Kessler et al., 1992; Meyer et al., 1991; Michaelis et al., 1998; Rivera et al., 2000), joints (Pinto et al., 2007), colonic tissue (Brumovsky et al., 2009; Feng and Gebhart, 2011; Su and Gebhart, 1998), the cornea (Parra et al., 2014), and the dura mater (Burstein et al., 1998b; Strassman et al., 1996). Almost unanimously, IS effectively activates and sensitizes primary afferent nociceptors, rendering them hyper-excitable, spontaneously active, and responsive to previously sub-threshold mechanical and thermal stimuli (Chen et al., 2007; Grossmann et al., 2009; Ma et al., 2006; Meyer et al., 1991; Michaelis et al., 1998).

We have previously shown that brief administration of IS to the anesthetized rat dura activates and sensitizes meningeal nociceptors to an extent that is sufficient to trigger sequential activation and sensitization of central trigeminovascular neurons in the spinal

trigeminal nucleus and sensory thalamus (Burstein et al., 1998b; Burstein et al., 2000a; Burstein et al., 2010; Strassman et al., 1996). These studies suggest that sensitization of meningeal nociceptors can explain the intensification of headache by mundane activities that momentarily increases intracranial pressure. This also suggests that sensitization of spinal trigeminovascular neurons can explain cephalic allodynia and pericranial muscle tenderness that develops after the onset of headache, and that sensitization of thalamic trigeminovascular neurons can explain the gradual development of extracephalic allodynia (Burstein et al., 2000d).

Accordingly, in this study, we sought to capture changes induced by the application of IS, to the dura mater across multiple brain networks - critical for establishing a reliable translational animal model of migraine chronification. To achieve this, rats were implanted with an epidural catheter in the space between the skull and the superior sagittal sinus. On the day of examination, initial administration of either sham, synthetic interstitial fluid (SIF), or IS was subsequently followed by conscious (awake) functional magnetic resonance imaging (fMRI). Our primary hypothesis was that IS induced animals would exhibit global changes in functional connectivity networks beyond the primary pain matrix brain regions compared to sham induced animals, similar to fMRI reports in clinical migraine populations. Additionally, we hypothesized that IS induced animals would show increased BOLD activation to both mechanical and thermal stimulation as compared to SIF induced, sham, animals, also consistent with clinical literature. To the best of our knowledge, this is the first study that has attempted to measure IS-induced changes in whole brain activity.

2. Results

One IS and one SIF rat was excluded from further analysis due to excessive motion (more than 0.5 mm), leaving 11 animals in each group for imaging analysis. Maximum displacements during MRI acquisition were utilized to compare IS vs. SIF infused rats as a behavioral pain indicator. For evoked mechanical stimulation IS rats showed a (mean±stdev) peak-displacement of 0.15±0.12 mm, SIF rats: 0.18±0.12 mm ($p=0.47$, t-test). For RSN scans, IS had 0.12±0.06 mm while SIF rats displayed 0.16±0.11 mm displacements ($p=0.31$, t-test). Accordingly, there was no indication that one group had increased motion due to the application of IS or SIF.

Evoked Thermal Stimulation: IS vs. SIF

Comparison of noxious thermal heat applied to the face of the rat resulted in no significant differences between the groups.

Evoked Mechanical Stimulation: IS vs. SIF

The activation map of evoked mechanical stimulation resulted in several significant activated areas comparing IS vs. SIF-treated rats (Figure 2 and Table 1); primary somatosensory areas contralateral to the stimulated area activated in primary somatosensory barrel field and dysgranular region. Sub cortically; caudate/putamen, hippocampus (CA1 and CA3), hypothalamus, amygdala, thalamus (ventro medial and ventro posterior lateral), periaqueductal gray, reticular formation, and cerebellar structures showed significantly

greater BOLD activation in IS rats compared to sham (SIF) animals. Conversely, only the retrosplenial cortex displayed decreased activity in the IS group.

Effects on Brain Networks

Administration of IS produced significant changes (as compared to SIF) in a number of networks Figure 3 and Table 2). For each network, changes in connectivity with respect to specific brain structures are noted in Table 2.

Default Mode Network (DMN)—The DMN displayed increased connectivity with the following cortical and subcortical areas: insula, cingulate, sensorimotor and perirhinal cortices, caudate/putamen, hypothalamus, posterior thalamus, amygdala, and hippocampus. This network displayed decreased connectivity only with cerebellum lobule 08.

Sensorimotor Network (SMN)—The SMN displayed increased connectivity with the somatosensory cortex, caudate putamen, rubral area and inferior colliculus; and decreased connectivity with secondary visual cortex and hippocampus.

Interoceptive (Salience) Network (SN)—The SN displayed increased connectivity with somatosensory and insular cortices, caudate putamen and hippocampus. This network displayed decreased connectivity with somatosensory cortex, reticular formation, fimbria-fornix, and cerebellum.

Autonomic Network (AN)—The autonomic network displayed increased connectivity with the amygdala and the hippocampus.

Basal Ganglia Networks (BGN)—Basal ganglia networks displayed increased connectivity with the secondary somatosensory, insula, visual, retrosplenial and temporal association cortices, and with caudate, putamen and amygdala. Decreased connectivity was observed with the olfactory cortex and simple lobule.

Cerebellum Network (CN)—Increased connectivity was observed with the insular, somatosensory and temporal association cortices, and with the amygdala, hypothalamus, and hippocampus. Decreased connectivity was observed with motor and visual cortices, sub cortically with caudate, putamen, hippocampus, medial ventral thalamus, and ansiform lobule crus 1.

Summary of IS vs. SIF Network alterations—IS-treated rats displayed mostly increases in connectivity for all identified brain networks as measured by relative regions involved in each network and volume of activation. Thus, the increases can be quantitated volumetrically as follows: DMN (93.11 mm^3), SMN (9.71 mm^3), SN (47.00 mm^3), AN (7.63 mm^3), BGN (25.69 mm^3), and CN (22.15 mm^3). Similarly, some networks display decreased connectivity and are also defined by volume of activation: DMN (1.26 mm^3), SMN (7.01 mm^3), SN (13.56 mm^3), BGN (3.13 mm^3), CN (10.48 mm^3).

3. Discussion

The current study provides the first fMRI evaluation of whole brain (network analysis) effects of dural exposure to IS. As shown earlier in a series of single-unit electrophysiological studies (Burstein et al., 1998b; Strassman et al., 1996), topical administration of IS to the dura enhanced responses to mechanical stimulation of the face in the spinal trigeminal nucleus and thalamus. Here, however, such enhanced responses (all indicative of sensitization, allodynia and hyperalgesia) were recorded in cortical and subcortical areas not previously reported. We also found that topical administration of IS to the dura of conscious rats produced changes in the default mode, salience, executive, basal ganglia, autonomic, and cerebellar networks. These changes are similar to those observed in migraine, as well as neuropathic pain patients (Tessitore et al., 2013; Tso et al., 2015; Xue et al., 2012; Xue et al., 2013). In general, we have observed an overall increase in connectivity in the IS group compared to the control, SIF group. The findings suggest that activation and sensitization of meningeal nociceptors by IS can (on its own) shift the animal into a state of neuronal hyper excitability, alter the effects of peripheral stimuli, and provide some indications that potentially enhances nociceptive processing.; define new level of modulation of affective and cognitive responses to pain. Additionally alterations to these networks may set a new tone for hypothalamic regulation of autonomic outflow to the cranium and change cerebellar functions. Taken together, these findings enhance our understanding and justify the ongoing use of IS to study the headache phase of migraine and many of its associated symptoms.

Evoked mechanical and thermal stimulation

Mechanical stimulation elicited a larger brain activation in IS rats as compared to SIF animals in cortical, subthalamic, hippocampal and hypothalamic areas – all areas not explored previously for their role in the cutaneous allodynia and hyperalgesia during migraine. These results, add complexity to the mechanisms that mediate the development of skin hypersensitivity during acute migraine attacks. In contrast, we did not anticipate the lack of enhanced response to thermal stimulation of the skin as clinical migraineurs exhibit heat allodynia during acute attacks (Burstein et al., 2000a; Burstein et al., 2000c). Furthermore, previous reports demonstrate that local administration of IS to the dura decreases response threshold and increases response magnitude to heat stimulation in 2nd and 3rd-order central trigeminovascular neurons ((Burstein et al., 1998a; Burstein et al., 2010). This discrepancy may reflect the time difference between our experimental design and those used previously. Migraine patients exhibit heat allodynia 2-4 hours after onset of migraine and thalamic neurons alter their response to heat stimuli hours after administration of IS. In contrast, our scans were taken shortly after IS application.

The Significance of Alteration in Brain Networks by Inflammatory Soup (IS)

The *Default Mode Network* represents a network that monitors the state of the subject and is important for processing emotions (Mittner et al., 2016; Mohan et al., 2016). Previous studies of common migraine patients in the interictal phase showed increased connectivity in the DMN with the anterior insula and decreased connectivity with prefrontal areas. (Tessitore et al., 2013; Xue et al., 2012). To the best of the authors' knowledge, there are no

reports of alterations of brain networks in general, and the DMN specifically, during a migraine attack and hence the published results are not directly comparable. Nevertheless, the alterations in the interictal phase likely are preserved if not exacerbated during a migraine attack. Here, the model intends to reflect the migraine state, yet, the fact that dural exposure to IS induced similar changes suggests that this stimulus is sufficient to derange the DMN (both within itself and with other structures).

The *Salience Network* is thought to play a key role in the evaluation of the state or condition of a threat to the organism (Borsook et al., 2013). Using almost identical methods, we showed recently that the salience network of clinical migraineurs exhibits increased connectivity with the primary somatosensory cortex (Maleki et al., 2012). The fact that dural exposure to IS induced similar changes in the awake rat suggests that local application of inflammatory soup to the dura, well beyond its ability to activate meningeal nociceptors, is capable of altering: (1) components of the salience network that determine the magnitude of the organism response to stimuli that originate inside the body (i.e., interoception) (Colder et al., 2013) and, (2) components of the sensorimotor network that determine the extent of enhanced nociceptive processing (i.e., neuronal firing to a given stimulus). We observed a region of the primary somatosensory cortex (jaw region) to display reduced connectivity with the salience network for IS vs. SIF. We speculate that such change might arise relating to the organization of the trigeminal system: The IS predominantly activates dural nociceptors in V1. The mechanism of the jaw region decreased connectivity with IS may be related to the concept of ‘lateral inhibition’ (Lo et al., 1999) at the level of the trigeminal nucleus (Burstein et al., 1998b) that is then reflected in higher order systems (connectivity changes); or possibly diminished effect of central sensitization (at a thalamic level (Burstein et al., 2010).

The *Basal Ganglia Network* is in a position to modulate sensory, affective, and cognitive responses to pain (Borsook et al., 2010). Based on our previous clinical migraine imaging studies, we observed profound functional and structural changes in the basal ganglia. Structurally, migraineurs exhibit a reduction in basal ganglia size (gray matter volume) while functionally it is less active in migraineurs than in control subjects. This effect is amplified in high frequency migraineurs showing both a further volumetric loss and diminished functional activity compared to low frequency migraineurs (Maleki et al., 2011). We also noticed that functional connectivity between the basal ganglia, insula, hippocampus, and temporal pole is increased when migraineurs are exposed to noxious stimuli (Maleki et al., 2011; Yuan et al., 2013). Accordingly, we interpreted the IS-induced increase in connectivity between the basal ganglia and the insula, retrosplenial cortex, and amygdala as suggesting that local administration of IS to the dura triggers changes in neural networks that are similar to those seen in migraine patients. These findings expand upon and support the validity of the IS rodent model of headache.

The *autonomic network* sets the balance between sympathetic and parasympathetic outflow (Shields, 1993). It is thought to originate in the hypothalamus (Dampney, 2011; Hosoya et al., 1983; Hosoya et al., 1984; Loewy, 1990; Tucker and Saper, 1985) and contribute to the variety of autonomic dysfunction seen in migraine (Alstadhaug, 2009; Goadsby, 2013). Supporting the notion of hypothalamic dysregulation is a previous imaging study in

migraineurs showing alterations in functional connectivity between the hypothalamus and brain regions that participate in regulating the firing of preganglionic sympathetic and parasympathetic neurons (Moulton et al., 2011). In agreement with the above statement, we found that topical application of IS to the dura resulted in decreased connectivity between the hypothalamus, amygdala, and hippocampus. This is the only result that seems to differ significantly from the human data. Nociceptive processing, like fear, is conserved across mammalian species (LeDoux, 2012). However, there may be differences on perception of "pain". Potential mechanisms may relate to the nature of the stimulus in the experimental paradigm vs. the clinical migraine state; although many functional similarities between rat and human brain function have been defined (Brunton et al., 2013; Clark and Squire, 2013), differences in brain systems in rats and humans where overall systems may be differentially regulated although baseline RSNs have been reported to be quite consistent across species (Becerra et al., 2011; Gozzi and Schwarz, 2016).

Migraine headaches associated with abnormal cerebellar anatomy (e.g., Chiari malformation) and function (e.g., dizziness, ataxia, poor motor coordination) are well documented (Kaplan and Oksuz, 2008; Russell and Ducros, 2011; Vincent and Hadjikhani, 2007), and convincingly evident by imaging studies that show multiple subclinical cerebellar infarct-like lesions in migraine aura patients (Kruit et al., 2004; Kruit et al., 2005; Kruit et al., 2010; Scher et al., 2009). In fact, cerebellar abnormalities in migraine have been elegantly demonstrated in translational genetic studies on familial hemiplegic migraine as well (Ferrari et al., 2015). It is therefore not surprising that our data identified IS-induced alterations in the *Cerebellum Network*. Reassuringly, the changes we observed in the rodent (i.e., increased connectivity with the insula, amygdala, hypothalamus, and hippocampus, and decreased connectivity with caudate/putamen) were similar to changes observed in migraine pain networks (Moulton et al., 2011) (Vincent and Hadjikhani, 2007).

Decreased connectivity in the *Sensorimotor Network* has been reported in clinical experimental pain (Flodin et al., 2014; Ter Minassian et al., 2013) and clinical pain (Cifre et al., 2012). Our interpretation is that the ongoing pain (4 hours) induced by the inflammatory soup produced results in activation of brain systems.

Although IS brain alterations are robust, it is important to note that these changes, may not be unique to the migraine condition and, in fact, might share similarities with other chronic pain conditions observed in humans (Baliki et al., 2014). To the best of the authors' knowledge, there are very few studies specifically investigating brain network alterations in chronic pain models. Though others have examined interhemispheric decreases in connectivity in models of neuropathic pain (Pawela et al., 2010) as well as changes in grey matter structure (Goncalves et al., 2008; Seminowicz et al., 2009). Further studies are warranted to tease apart the characteristics of the IS model that are unique to the migraine condition from other, more broad, chronic pain pathology.

Caveats

There are a several caveats that warrant consideration:

1. *The Model:* The model is a single “attack” and may not represent ongoing changes associated with repeated attacks observed in most episodic migraineurs. However, the model, as noted in the introduction, does provide parallel expression of a number of processes that are observed in the human (Burstein et al., 1998b; Burstein et al., 2004; Burstein et al., 2010) including reversal of some processes, particularly somatosensory ones. Furthermore, the issue of inflammatory processes can be considered in the following manner: (1) local inflammation that activates nociceptive processes as assessed by electrophysiological measures of trigeminal system afferents (Levy et al., 2007; Oshinsky, 2014; Strassman et al., 1996); and (2) more diffuse effects of the inflammation on brain systems (ref). There are a number of approaches to evaluating the latter including: (a) direct measures of inflammatory systems using PET markers of glial activity (Ji et al., 2013; Loggia et al., 2015; Owen and Matthews, 2011)with and without IS application; and (b) measures of CSF markers of inflammation (viz., cytokines (Bakhiet et al., 1998) or other markers of neuroimmune activation (viz., neopterin (Murr et al., 2002).

2. *Animals:* In this study we only used male rats, however, we are aware that the human migraine condition is significantly biased towards females. Given the nature of controlling for menstrual cycle, our first study aimed at using models that have previously been reported in the literature where male rats were used (Levy et al., 2004). Having established the fMRI approach, a similar study carried out in a female cohort should be performed to investigate the role of sex and chronic migraine (Oshinsky et al., 2012).

3. *Imaging:* Unfortunately, anesthesia substantially suppresses neural activity providing a rationale for neuroimaging to be conducted in awake animals. Undoubtedly there may be stress and anxiety associated with the conscious imaging procedure and restraint, although we attempted to mitigate these effects by acclimating the animals to the MRI prior to experimentation. Additionally, we can not completely disregard possible effects of anesthesia, of which there is now supportive data that indicates can profoundly affect emotional circuits, and to a lesser extent sensory circuits (Liang et al., 2015). However, both groups were exposed to identical levels and timeframes of anesthetic.

4. Conclusions

This paper addresses the use of fMRI in translational migraine research, emphasizing that the data previously collected in the IS model can be evaluated using whole brain functional neuroimaging. It also provides a model to evaluate acute and chronic effects on brain systems in a rodent model. Furthermore, the translational validity is supported by similar findings in both humans and a rodent model that has been characterized to have a number of pathological parallels.

5. Materials and Methods

Experimental Design

The study was approved by the Massachusetts General Hospital Institutional Animal Care and Use Committee (IACUC). Twenty-four male Sprague-Dawley rats (Charles River Lab, Wilmington, MA), 8 weeks of age and weighing approximately 300-350 grams, were used for these experiments. MRI acclimated animals underwent a surgical procedure to implant a catheter just deep to the skull. Twelve animals received an injection (20μL) of inflammatory soup and twelve animals were administered a control vehicle (synthetic interstitial fluid: SIF) (Strassman et al., 1996) followed by subsequent conscious resting state, thermal, and mechanical fMRI.

MRI Acclimation—To increase specificity of acquired images to dural stimulation with IS or SIF, and mitigate stress and anxiety responses, rats were first acclimated to the imaging cradle and head gear apparatus during three consecutive training sessions (days 1, 2 and 3). In each session, rats were lightly anesthetized with 2% Isoflurane, positioned into custom MRI body cradles and imaging head gear, and placed in a mock MRI box for 1 hour. During this time the animals were exposed to the full range of MRI sounds performed on the day of data collection.

Dural Cannulation

On day 3 (after the final MRI acclimation session), rats underwent a surgical procedure to implant an indwelling cannula on top of the dura. Animals were first anesthetized with 2% isoflurane followed by a single IP injection of a mixture of ketamine (50 mg/kg), Xylazine (5 mg/Kg), and Acepromazine (1 mg/Kg) and subsequent subcutaneous injection of Atropine (0.1 mg/ml). Each animal was head-fixed utilizing a stereotaxic device and wrapped in a circulating water heating pad to maintain physiological temperature. A small incision was made in a rostral to caudal direction to expose the skull and more specifically the lambda and bregma cranial sutures. Using a surgical microscope and micro drill, a small graded trough was made parallel and lateral to the sagittal suture, on the right side, exposing the dura just anteriorly to the lambda suture. A PE-10 cannula (PE 10) was then inserted into the trough, lateral to superior sagittal sinus between Lambda and Bregma cranial sutures. Caution was taken to ensure that the cannula was placed on top of the dura without damaging the meningeal tissue. The cannula was then secured in place to the skull using dental cement, threaded under the skin and extended out of a small incision at the anterior portion of the face, superior and medial to the whisker pad. The exterior portion of the tubing was heat-sealed to prevent infection and to allow injection of IS or SIF on the day of imaging.

Dural Stimulation

On experimental day five, the cannula was trimmed several millimeters to remove the heat seal and enable injection of SIF or IS. 20 μL of solution (IS or SIF) was then administered topically onto the dura through the implanted cannula over a 20 second interval (~1 μL/s), 90 minutes prior to the start of functional imaging. The IS solution contained 1 mM histamine, 1 mM serotonin, 1 mM bradykinin, and 0.1 mM prostaglandin E_2 (pH 5.5). The

modified SIF contained 135 mM NaCl, 5 mM KCl, 1 mM $MgCl_2$, 5 mM $CaCl_2$, 10 mM glucose and 10 mM Hepes (pH 7.2). Following injection, the tubing was once again heat sealed using glass-bead sterilized forceps to ensure that there was no loss of either SIF or IS.

Conscious MRI Setup

One hour following dural stimulation, rats were briefly anesthetized (2% Isoflurane for 15 minutes) to allow positioning of a custom made MRI body cradle and ear bars that fit in the depression between the angle of the mandible and the anterior border of the sternocleidomastoid muscle. Headgear with a bite bar was then positioned over the ear bars and finally placed in a larger, open tubular apparatus that secured the headgear and prevented head motion. The ear bars were designed to be adjustable enabling them to remain in place without causing discomfort to the animal. Next, thermal and mechanical stimulation equipment was unilaterally affixed to the shaved whisker pad on the right side, followed by placement of an in-house-built MRI surface coil. Animals were then positioned into the MRI scanner for image acquisition.

MRI Acquisition

Once awake, anatomical images were acquired with a RARE sequence (24 1.0 mm slices, TR/TE = 4000/40.5 ms, 128×128 in-plane resolution with FOV of 30 mm) in a 4.7 T Bruker BioSpec Scanner (Bruker, Billerica, MA). At 90 minutes post-IS/SIF infusion, a Resting State Scan (RSN) was acquired with an EPI sequence: (15 Slices 1.5 mm thick, TR/TE = 3000/12 ms, FOV: 3cm, 64×64, 90 time points). The resting state network (RSN) scans were followed by two functional scans; the first was acquired during repeated mechanical stimulation of the facial skin with a nylon filament and the second during repeated noxious heat stimulation (Figure 1). A block design was used for both stimulation paradigms with 27 seconds rest (6 epochs) and 21 seconds stimulation (5 epochs). Total imaging time was approximately 90 minutes.

Mechanical and Thermal Stimulation

Setup of the equipment took place while the rat was under anesthesia and loaded into the MRI cradle for imaging. A specially constructed apparatus controllable outside of the MRI, allowed the facial stimulation of the rat through thermal contact and mechanical punctuate stimulation (Figure 1). Thermal stimulation was delivered by a narrow solid copper rod (5mm diameter solid copper block tapered for optimal skin contact and internally bathed with circulating water to achieve the desired temperature) that was set against the shaved whisker barrel field, adjacent to the trigeminal mesencephalic nucleus of the ipsilateral side of the IS/SIF injection. A thermocouple was glued to the tip of the copper rod to monitor temperature. Five, 21 second noxious stimuli were applied at 48°C and delivered in a block design with 27 second interval spacing. To perform mechanical stimulation, a thin plastic tube with a curved end was attached alongside the copper block used to deliver the thermal stimuli, enabling it to point perpendicular to the whisker barrel of the rat. A nylon fiber was threaded through the tube and the limits of its displacement were set so that it produced a noticeable indentation of the face with a force of approximately 30g. Additionally, to prevent possible study bias, the investigators running the MRI sessions were blinded to the experimental group of each animal.

Mechanical and Thermal Stimulation Analysis

Evoked fMRI images were processed as previously described (Becerra et al., 2011) with fsl 4.1.9 (fmrib/fsl.html). In brief, images underwent motion correction utilizing fsl's MCFLIRT algorithm and spike detection using the *fsl_motion_outliers* script. MCFLIRT uses the middle timepoint image as the reference and performs rigid-body alignment of the other times points to this image. The transformation matrix is converted to 6 measurements (3 rotations and 3 translations). The average displacement is then calculated for each animal. Animals exhibiting more than 0.5 mm displacement were excluded from the study. Mean displacement comparisons between the 2 groups were statistically tested using a Student's t-test. Next, manual brain extraction was implemented to isolate brain tissue from the skull and non-brain soft tissue. Six motion correction parameters and a single spike detection explanatory variable were used as regressors of non interest to clean the data. The cleaned data was then spatially smoothed using a Gaussian Kernel FWHM of 0.7 mm filter and high-pass filtered with a 0.01 Hz threshold. A generalized linear model approach was used with an explanatory variable (EV) that modeled the temporal profile of the stimuli (mechanical or thermal). The final EV resulted from the convolution with a gamma function as calculated by fsl. Group differences between IS and SIF was calculated using a random model approach as instituted in fsl. Statistical significance was determined with a false-discovery-rate enhanced mixture model approach (Pendse et al., 2009).

RSN Analysis

RSN data was pre-processed similarly to the evoked stimuli paradigm described above including a HPF threshold of 0.01 Hz (Becerra et al. 2011). Independent component analysis (ICA) was run at the individual level and inspected for components with temporal profiles that resemble motion correction plots. Individual components were further spatially inspected to confirm motion-related nature (e.g. edge effect activity). These components were removed utilizing fsl tools (fslreg). De-noised data were then concatenated and an ICA-based group decomposition calculated to determine 40 components using FSL's melodic tool.

Network Identification

Networks for healthy rats, previously described in the literature (Becerra et al., 2011), including the cerebellar, default mode network, basal ganglia loops, sensorimotor and autonomic networks, were used as templates for component identification from the total group ICA decomposition. A spatial Pearson correlation coefficient was calculated between each component and the templates to quantify goodness-of-fit. Correlation coefficients larger than 0.25 were considered significant and were used to determine correspondence between components and specific RSN templates. Components with a correlation coefficient greater than 0.25 were visually inspected to confirm similarity with published data. RSN scans were then processed with a dual regression approach to determine changes in co-activation of whole brain with identified networks (Filippini et al., 2009). Group statistical maps for each component were determined with a randomized approach (Filippini et al., 2009) and statistical significance accounting for multiple comparisons was determined with

a combined mixture-model and false discovery rate method (Pendse et al, 2009). The resulting identified networks are displayed in Figure 3.

Calculating a Pearson correlation coefficient between the 40 components identified the networks described.

In addition, components that did not display a general pattern reflecting a network of neurological origin (i.e., brain areas not near CSF of mayor vessels) were excluded of further analysis. Such components may carry residual motion as well as physiological artifacts.

Acknowledgments

Migraine Research Foundation (DB). Louis Herlands Fund for Pain Research (DB, LB). GlaxoSmithKline (Investigator Initiated Grant) (RB), and NIH grants NS069847 (RB), NS079678 (RB), K24-NS064050 (DB).

References

Alstadhaug KB. Migraine and the hypothalamus. Cephalalgia. 2009; 29:809–17. [PubMed: 19604254]

Bahra A, Matharu MS, Buchel C, Frackowiak RS, Goadsby PJ. Brainstem activation specific to migraine headache. Lancet. 2001; 357:1016–7. [PubMed: 11293599]

Bakhiet M, Mustafa M, Zhu J, Harris R, Lindquist L, Link H, Diab A. Induction of cytokines and anti-cytokine autoantibodies in cerebrospinal fluid (CSF) during experimental bacterial meningitis. Clin Exp Immunol. 1998; 114:398–402. [PubMed: 9844049]

Baliki MN, Mansour AR, Baria AT, Apkarian AV. Functional reorganization of the default mode network across chronic pain conditions. PLoS One. 2014; 9:e106133. [PubMed: 25180885]

Becerra L, Pendse G, Chang PC, Bishop J, Borsook D. Robust reproducible resting state networks in the awake rodent brain. PLoS One. 2011; 6:e25701. [PubMed: 22028788]

Borsook D, Upadhyay J, Chudler EH, Becerra L. A key role of the basal ganglia in pain and analgesia–insights gained through human functional imaging. Mol Pain. 2010; 6:27. [PubMed: 20465845]

Borsook D, Edwards R, Elman I, Becerra L, Levine J. Pain and analgesia: the value of salience circuits. Prog Neurobiol. 2013; 104:93–105. [PubMed: 23499729]

Brumovsky PR, Feng B, Xu L, McCarthy CJ, Gebhart GF. Cystitis increases colorectal afferent sensitivity in the mouse. Am J Physiol Gastrointest Liver Physiol. 2009; 297:G1250–8. [PubMed: 19779012]

Brunton BW, Botvinick MM, Brody CD. Rats and humans can optimally accumulate evidence for decision-making. Science. 2013; 340:95–8. [PubMed: 23559254]

Burstein R, Yamamura H, Malick A, Strassman AM. Chemical stimulation of the intracranial dura induces enhanced responses to facial stimulation in brain stem trigeminal neurons. Journal of Neurophysiology. 1998a; 79:964–982. [PubMed: 9463456]

Burstein R, Yamamura H, Malick A, Strassman AM. Chemical stimulation of the intracranial dura induces enhanced responses to facial stimulation in brain stem trigeminal neurons. J Neurophysiol. 1998b; 79:964–82. [PubMed: 9463456]

Burstein R, Cutrer FM, Yarnitsky D. The development of cutaneous allodynia during a migraine attack: clinical evidence for the sequential recruitment of spinal and supraspinal nociceptive neurons in migraine. Brain. 2000a; 123:1703–1709. [PubMed: 10908199]

Burstein R, Cutrer MF, Yarnitsky D. The development of cutaneous allodynia during a migraine attack clinical evidence for the sequential recruitment of spinal and supraspinal nociceptive neurons in migraine. Brain. 2000b; 123(Pt 8):1703–9. [PubMed: 10908199]

Burstein R, Yarnitsky D, Goor-Aryeh I, Ransil BJ, Bajwa ZH. An association between migraine and cutaneous allodynia. Annals Neurol. 2000c; 47:614–624.

Burstein R, Yarnitsky D, Goor-Aryeh I, Ransil BJ, Bajwa ZH. An association between migraine and cutaneous allodynia. Ann Neurol. 2000d; 47:614–24. [PubMed: 10805332]

Burstein R, Collins B, Jakubowski M. Defeating migraine pain with triptans: a race against the development of cutaneous allodynia. Ann Neurol. 2004; 55:19–26. [PubMed: 14705108]

Burstein R, Jakubowski M, Garcia-Nicas E, Kainz V, Bajwa Z, Hargreaves R, Becerra L, Borsook D. Thalamic sensitization transforms localized pain into widespread allodynia. Ann Neurol. 2010; 68:81–91. [PubMed: 20582997]

Chen X, Alessandri-Haber N, Levine JD. Marked attenuation of inflammatory mediator-induced C-fiber sensitization for mechanical and hypotonic stimuli in TRPV4−/− mice. Mol Pain. 2007; 3:31. [PubMed: 17967183]

Cifre I, Sitges C, Fraiman D, Munoz MA, Balenzuela P, Gonzalez-Roldan A, Martinez-Jauand M, Birbaumer N, Chialvo DR, Montoya P. Disrupted functional connectivity of the pain network in fibromyalgia. Psychosom Med. 2012; 74:55–62. [PubMed: 22210242]

Clark RE, Squire LR. Similarity in form and function of the hippocampus in rodents, monkeys, and humans. Proc Natl Acad Sci U S A. 2013; 110(Suppl 2):10365–70. [PubMed: 23754372]

Colder CR, Hawk LW Jr, Lengua LJ, Wiezcorek W, Eiden RD, Read JP. Trajectories of Reinforcement Sensitivity During Adolescence and Risk for Substance Use. J Res Adolesc. 2013; 23:345–356. [PubMed: 23772169]

Coppola G, Schoenen J. Cortical excitability in chronic migraine. Curr Pain Headache Rep. 2012; 16:93–100. [PubMed: 22076672]

Dampney, RA. The hypothalamus and autonomic regulation: An overview In Central regulation of autonomic functions. Llewellyn-Smith, IJ., Verberne, AJM., editors. oxford; New York: 2011. p. 47-61.

De Felice M, Eyde N, Dodick D, Dussor GO, Ossipov MH, Fields HL, Porreca F. Capturing the aversive state of cephalic pain preclinically. Ann Neurol. 2013; 74:257–65. [PubMed: 23686557]

Feng B, Gebhart GF. Characterization of silent afferents in the pelvic and splanchnic innervations of the mouse colorectum. Am J Physiol Gastrointest Liver Physiol. 2011; 300:G170–80. [PubMed: 21071510]

Ferrari MD, Klever RR, Terwindt GM, Ayata C, van den Maagdenberg AM. Migraine pathophysiology: lessons from mouse models and human genetics. Lancet Neurol. 2015; 14:65–80. [PubMed: 25496898]

Filippini N, MacIntosh BJ, Hough MG, Goodwin GM, Frisoni GB, Smith SM, Matthews PM, Beckmann CF, Mackay CE. Distinct patterns of brain activity in young carriers of the APOE-epsilon4 allele. Proc Natl Acad Sci U S A. 2009; 106:7209–14. [PubMed: 19357304]

Flodin P, Martinsen S, Lofgren M, Bileviciute-Ljungar I, Kosek E, Fransson P. Fibromyalgia is associated with decreased connectivity between pain-and sensorimotor brain areas. Brain Connect. 2014; 4:587–94. [PubMed: 24998297]

Goadsby PJ. Autonomic nervous system control of the cerebral circulation. Handb Clin Neurol. 2013; 117:193–201. [PubMed: 24095126]

Goncalves L, Silva R, Pinto-Ribeiro F, Pego JM, Bessa JM, Pertovaara A, Sousa N, Almeida A. Neuropathic pain is associated with depressive behaviour and induces neuroplasticity in the amygdala of the rat. Exp Neurol. 2008; 213:48–56. [PubMed: 18599044]

Gozzi A, Schwarz AJ. Large-scale functional connectivity networks in the rodent brain. Neuroimage. 2016; 127:496–509. [PubMed: 26706448]

Grossmann L, Gorodetskaya N, Baron R, Janig W. Enhancement of ectopic discharge in regenerating A- and C-fibers by inflammatory mediators. J Neurophysiol. 2009; 101:2762–74. [PubMed: 19279148]

Hosoya Y, Matsushita M, Sugiura Y. A direct hypothalamic projection to the superior salivatory nucleus neurons in the rat. A study using anterograde autoradiographic and retrograde HRP methods. Brain Res. 1983; 266:329–33. [PubMed: 6191826]

Hosoya Y, Matsushita M, Sugiura Y. Hypothalamic descending afferents to cells of origin of the greater petrosal nerve in the rat, as revealed by a combination of retrograde HRP and anterograde autoradiographic techniques. Brain Res. 1984; 290:141–5. [PubMed: 6692130]

Ji RR, Berta T, Nedergaard M. Glia and pain: is chronic pain a gliopathy? Pain. 2013; 154(Suppl 1):S10–28. [PubMed: 23792284]

Kaplan Y, Oksuz E. Chronic migraine associated with the Chiari type 1 malformation. Clin Neurol Neurosurg. 2008; 110:818–22. [PubMed: 18603356]

Katz EJ, Gold MS. Inflammatory hyperalgesia: a role for the C-fiber sensory neuron cell body? J Pain. 2006; 7:170–8. [PubMed: 16516822]

Kessler W, Kirchhoff C, Reeh PW, Handwerker HO. Excitation of cutaneous afferent nerve endings in vitro by a combination of inflammatory mediators and conditioning effect of substance. P Exp Brain Res. 1992; 91:467–76. [PubMed: 1282891]

Kruit MC, van Buchem MA, Hofman PA, Bakkers JT, Terwindt GM, Ferrari MD, Launer LJ. Migraine as a risk factor for subclinical brain lesions. JAMA. 2004; 291:427–34. [PubMed: 14747499]

Kruit MC, Launer LJ, Ferrari MD, van Buchem MA. Infarcts in the posterior circulation territory in migraine. The population-based MRI CAMERA study. Brain. 2005; 128:2068–77. [PubMed: 16006538]

Kruit MC, van Buchem MA, Launer LJ, Terwindt GM, Ferrari MD. Migraine is associated with an increased risk of deep white matter lesions, subclinical posterior circulation infarcts and brain iron accumulation: the population-based MRI CAMERA study. Cephalalgia. 2010; 30:129–36. [PubMed: 19515125]

LeDoux JE. Evolution of human emotion: a view through fear. Prog Brain Res. 2012; 195:431–42. [PubMed: 22230640]

Levy D, Jakubowski M, Burstein R. Disruption of communication between peripheral and central trigeminovascular neurons mediates the antimigraine action of 5HT 1B/1D receptor agonists. Proc Natl Acad Sci U S A. 2004; 101:4274–9. [PubMed: 15016917]

Levy D, Burstein R, Kainz V, Jakubowski M, Strassman AM. Mast cell degranulation activates a pain pathway underlying migraine headache. Pain. 2007; 130:166–76. [PubMed: 17459586]

Liang Z, Liu X, Zhang N. Dynamic resting state functional connectivity in awake and anesthetized rodents. Neuroimage. 2015; 104:89–99. [PubMed: 25315787]

Liu J, Zhao L, Lei F, Zhang Y, Yuan K, Gong Q, Liang F, Tian J. Disrupted resting-state functional connectivity and its changing trend in migraine suffers. Hum Brain Mapp. 2015; 36:1892–907. [PubMed: 25640857]

Lo FS, Guido W, Erzurumlu RS. Electrophysiological properties and synaptic responses of cells in the trigeminal principal sensory nucleus of postnatal rats. J Neurophysiol. 1999; 82:2765–75. [PubMed: 10561443]

Loewy, AD. Central autonomic pathways In Central regulation of autonomic functions. Loewy, AD., Spyer, KM., editors. Oxford University Press; Oxford: 1990.

Loggia ML, Chonde DB, Akeju O, Arabasz G, Catana C, Edwards RR, Hill E, Hsu S, Izquierdo-Garcia D, Ji RR, Riley M, Wasan AD, Zurcher NR, Albrecht DS, Vangel MG, Rosen BR, Napadow V, Hooker JM. Evidence for brain glial activation in chronic pain patients. Brain. 2015; 138:604–15. [PubMed: 25582579]

Ma C, Greenquist KW, Lamotte RH. Inflammatory mediators enhance the excitability of chronically compressed dorsal root ganglion neurons. J Neurophysiol. 2006; 95:2098–107. [PubMed: 16381809]

Maleki N, Becerra L, Nutile L, Pendse G, Brawn J, Bigal M, Burstein R, Borsook D. Migraine attacks the Basal Ganglia. Mol Pain. 2011; 7:71. [PubMed: 21936901]

Maleki N, Becerra L, Brawn J, Bigal M, Burstein R, Borsook D. Concurrent functional and structural cortical alterations in migraine. Cephalalgia. 2012; 32:607–20. [PubMed: 22623760]

Meyer RA, Davis KD, Cohen RH, Treede RD, Campbell JN. Mechanically insensitive afferents (MIAs) in cutaneous nerves of monkey. Brain Res. 1991; 561:252–61. [PubMed: 1802341]

Michaelis M, Vogel C, Blenk KH, Arnarson A, Janig W. Inflammatory mediators sensitize acutely axotomized nerve fibers to mechanical stimulation in the rat. J Neurosci. 1998; 18:7581–7. [PubMed: 9736675]

Mittner M, Hawkins GE, Boekel W, Forstmann BU. A Neural Model of Mind Wandering. Trends Cogn Sci. 2016; 20:570–8. [PubMed: 27353574]

Mohan A, Roberto AJ, Mohan A, Lorenzo A, Jones K, Carney MJ, Liogier-Weyback L, Hwang S, Lapidus KA. The Significance of the Default Mode Network (DMN) in Neurological and Neuropsychiatric Disorders: A Review. Yale J Biol Med. 2016; 89:49–57. [PubMed: 27505016]

Moulton EA, Becerra L, Maleki N, Pendse G, Tully S, Hargreaves R, Burstein R, Borsook D. Painful heat reveals hyperexcitability of the temporal pole in interictal and ictal migraine States. Cereb Cortex. 2011; 21:435–48. [PubMed: 20562317]

Murr C, Widner B, Wirleitner B, Fuchs D. Neopterin as a marker for immune system activation. Curr Drug Metab. 2002; 3:175–87. [PubMed: 12003349]

Oshinsky ML, Gomonchareonsiri S. Episodic dural stimulation in awake rats: a model for recurrent headache. Headache. 2007; 47:1026–36. [PubMed: 17635594]

Oshinsky ML, Sanghvi MM, Maxwell CR, Gonzalez D, Spangenberg RJ, Cooper M, Silberstein SD. Spontaneous trigeminal allodynia in rats: a model of primary headache. Headache. 2012; 52:1336–49. [PubMed: 22963523]

Oshinsky ML. Sensitization and ongoing activation in the trigeminal nucleus caudalis. Pain. 2014; 155:1181–2. [PubMed: 24708991]

Owen DR, Matthews PM. Imaging brain microglial activation using positron emission tomography and translocator protein-specific radioligands. Int Rev Neurobiol. 2011; 101:19–39. [PubMed: 22050847]

Parra A, Gonzalez-Gonzalez O, Gallar J, Belmonte C. Tear fluid hyperosmolality increases nerve impulse activity of cold thermoreceptor endings of the cornea. Pain. 2014; 155:1481–91. [PubMed: 24785271]

Pawela CP, Biswal BB, Hudetz AG, Li R, Jones SR, Cho YR, Matloub HS, Hyde JS. Interhemispheric neuroplasticity following limb deafferentation detected by resting-state functional connectivity magnetic resonance imaging (fcMRI) and functional magnetic resonance imaging (fMRI). Neuroimage. 2010; 49:2467–78. [PubMed: 19796693]

Pendse G, Borsook D, Becerra L. Enhanced false discovery rate using Gaussian mixture models for thresholding fMRI statistical maps. Neuroimage. 2009; 47:231–61. [PubMed: 19269334]

Pinto M, Lima D, Tavares I. Neuronal activation at the spinal cord and medullary pain control centers after joint stimulation: a c-fos study in acute and chronic articular inflammation. Neuroscience. 2007; 147:1076–89. [PubMed: 17590519]

Rivera L, Gallar J, Pozo MA, Belmonte C. Responses of nerve fibres of the rat saphenous nerve neuroma to mechanical and chemical stimulation: an in vitro study. J Physiol. 2000; 527(Pt 2): 305–13. [PubMed: 10970431]

Romero-Reyes M, Akerman S. Update on animal models of migraine. Curr Pain Headache Rep. 2014; 18:462. [PubMed: 25260835]

Russell MB, Ducros A. Sporadic and familial hemiplegic migraine: pathophysiological mechanisms, clinical characteristics, diagnosis, and management. Lancet Neurol. 2011; 10:457–70. [PubMed: 21458376]

Russo A, Tessitore A, Giordano A, Corbo D, Marcuccio L, De Stefano M, Salemi F, Conforti R, Esposito F, Tedeschi G. Executive resting-state network connectivity in migraine without aura. Cephalalgia. 2012; 32:1041–8. [PubMed: 22908362]

Scher AI, Gudmundsson LS, Sigurdsson S, Ghambaryan A, Aspelund T, Eiriksdottir G, van Buchem MA, Gudnason V, Launer LJ. Migraine headache in middle age and late-life brain infarcts. JAMA. 2009; 301:2563–70. [PubMed: 19549973]

Seminowicz DA, Laferriere AL, Millecamps M, Yu JS, Coderre TJ, Bushnell MC. MRI structural brain changes associated with sensory and emotional function in a rat model of long-term neuropathic pain. Neuroimage. 2009; 47:1007–14. [PubMed: 19497372]

Shields RW Jr. Functional anatomy of the autonomic nervous system. J Clin Neurophysiol. 1993; 10:2–13. [PubMed: 8458993]

Steen KH, Reeh PW, Anton F, Handwerker HO. Protons selectively induce lasting excitation and sensitization to mechanical stimulation of nociceptors in rat skin, in vitro. J Neurosci. 1992; 12:86–95. [PubMed: 1309578]

Steen KH, Steen AE, Reeh PW. A dominant role of acid pH in inflammatory excitation and sensitization of nociceptors in rat skin, in vitro. J Neurosci. 1995; 15:3982–3989. [PubMed: 7751959]

Steen KH, Steen AE, Kreysel HW, Reeh PW. Inflammatory mediators potentiate pain induced by experimental tissue acidosis. Pain. 1996; 66:163–70. [PubMed: 8880837]

Storer RJ, Supronsinchai W, Srikiatkhachorn A. Animal models of chronic migraine. Curr Pain Headache Rep. 2015; 19:467. [PubMed: 25416460]

Strassman AM, Raymond SA, Burstein R. Sensitization of meningeal sensory neurons and the origin of headaches. Nature. 1996; 384:560–4. [PubMed: 8955268]

Su X, Gebhart GF. Mechanosensitive pelvic nerve afferent fibers innervating the colon of the rat are polymodal in character. J Neurophysiol. 1998; 80:2632–44. [PubMed: 9819269]

Ter Minassian A, Ricalens E, Humbert S, Duc F, Aube C, Beydon L. Dissociating anticipation from perception: Acute pain activates default mode network. Hum Brain Mapp. 2013; 34:2228–43. [PubMed: 22438291]

Tessitore A, Russo A, Giordano A, Conte F, Corbo D, De Stefano M, Cirillo S, Cirillo M, Esposito F, Tedeschi G. Disrupted default mode network connectivity in migraine without aura. J Headache Pain. 2013; 14:89. [PubMed: 24207164]

Tso AR, Trujillo A, Guo CC, Goadsby PJ, Seeley WW. The anterior insula shows heightened interictal intrinsic connectivity in migraine without aura. Neurology. 2015; 84:1043–50. [PubMed: 25663219]

Tucker DC, Saper CB. Specificity of spinal projections from hypothalamic and brainstem areas which innervate sympathetic preganglionic neurons. Brain Res. 1985; 360:159–64. [PubMed: 4075168]

Vincent M, Hadjikhani N. The cerebellum and migraine. Headache. 2007; 47:820–33. [PubMed: 17578530]

Xue T, Yuan K, Zhao L, Yu D, Zhao L, Dong T, Cheng P, von Deneen KM, Qin W, Tian J. Intrinsic brain network abnormalities in migraines without aura revealed in resting-state fMRI. PLoS One. 2012; 7:e52927. [PubMed: 23285228]

Xue T, Yuan K, Cheng P, Zhao L, Zhao L, Yu D, Dong T, von Deneen KM, Gong Q, Qin W, Tian J. Alterations of regional spontaneous neuronal activity and corresponding brain circuit changes during resting state in migraine without aura. NMR Biomed. 2013; 26:1051–8. [PubMed: 23348909]

Yuan K, Zhao L, Cheng P, Yu D, Zhao L, Dong T, Xing L, Bi Y, Yang X, von Deneen KM, Liang F, Gong Q, Qin W, Tian J. Altered structure and resting-state functional connectivity of the basal ganglia in migraine patients without aura. J Pain. 2013; 14:836–44. [PubMed: 23669074]

Highlights

- This manuscript describes, for the first time, brain network alterations in the inflammatory soup model of migraine.
- We found that several brain networks are altered in the model compared to controls and that some of those alterations are similar to those observed in patients suffering of migraine.
- We also further provide experimental evidence that the model induces alterations in brain responses to mechanical stimulations producing an enhanced fMRI activity as compared to controls.

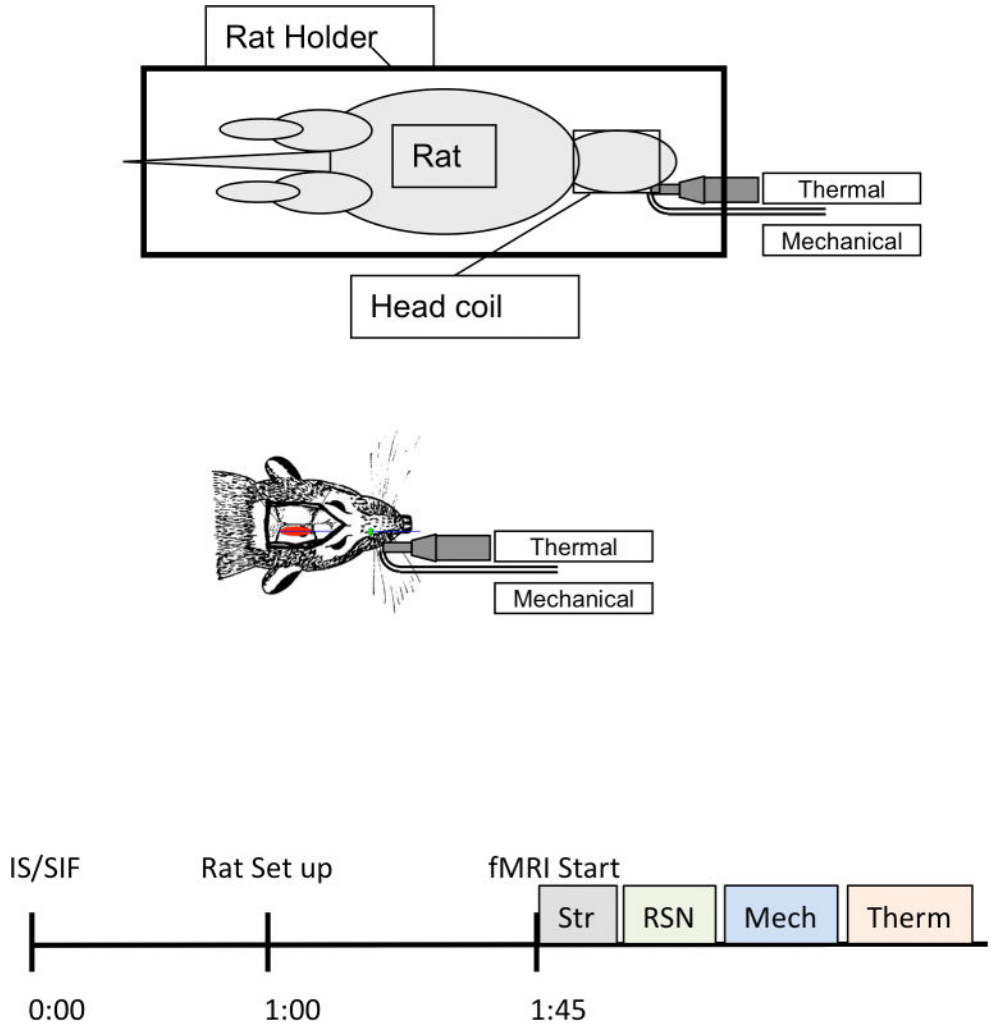

Figure 1. Experimental Design

Top of the figure displays a schematic of the unit utilized to deliver thermal and mechanical stimulation to the face of the rat. The unit did not cause artifacts on the MRI images. The rat was immobilized as described elsewhere (Becerra et al., 2011). The Middle panel depicts the position the cannula over the dura (red) and the exit port for IS/SIF administration (green). The details of how the thermal and mechanical unit were placed are also displayed. Bottom panel indicates the timing of the experimental procedure; after administration of IS or SIF, rats were returned to their cages for 1 hour before being prepare for the scan. After loading them on the MRI cradle under anesthesia, they were left to recover from anesthesia. Functional MRI studies started 45 minutes after loading of the rat. The imaging sessions started with a structural (Str) scan, 3 fMRI scans were acquired, the first a resting state scan (RSN) followed by evoked mechanical and thermal stimulation of the face.

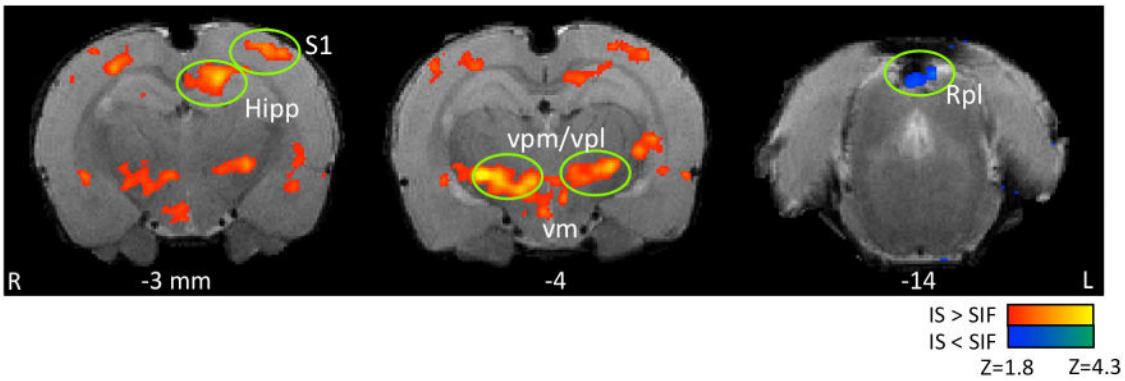

Figure 2. Evoked Mechanical Stimulation Brain Activation

The Figure displays some brain areas with statistically significant increased brain response to mechanical stimulation when comparing IS vs. SIF-treated rats. Only one brain area, retrosplenial cortex, displayed less activity in the IS rats compared to SIF. All areas of activation are listed in Table 1. Key: Hipp: Hippocampus, S1: somatosensory cortex-barrel field, vpm/vpl: thalamic ventro posterior medial and lateral nuclei, vm, ventro medial, Rpl: retrosplenial cortex.

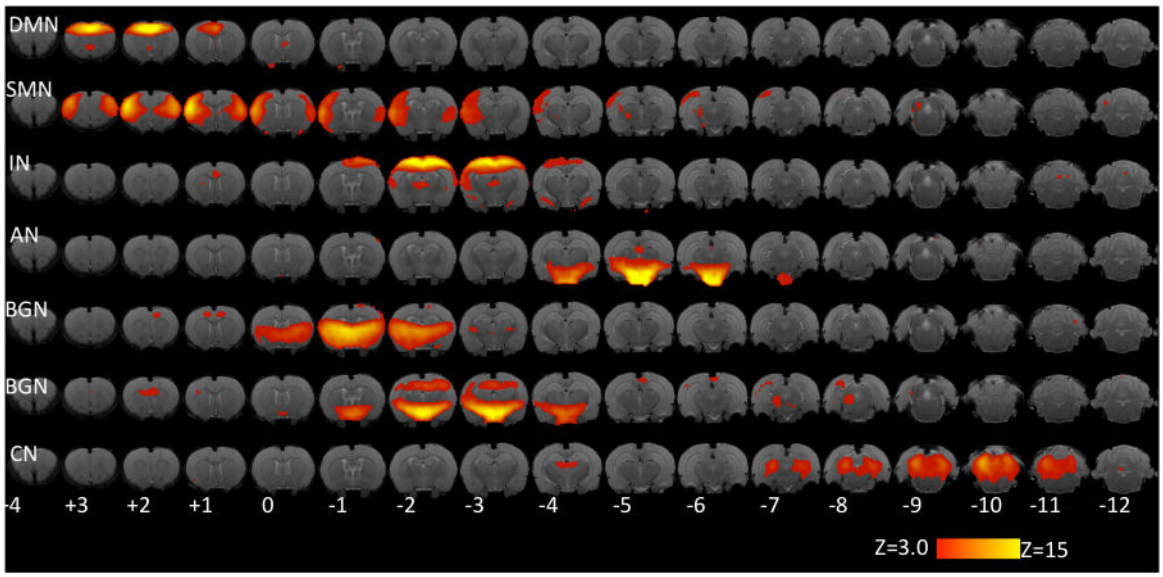

Figure 3. Resting State Networks

Networks identified in the IS+SIF analysis from a comparison with published networks in healthy rats (Becerra et al., 2011). Key: DMN: Default Mode Network. SMN: sensorimotor network. IN: interoceptive (salience) network. AN: autonomic network. BGN: Basal ganglia networks. CN: cerebellar network. Numbers indicate distance from bregma (in mm). Color code corresponds to the values of z-statistic.

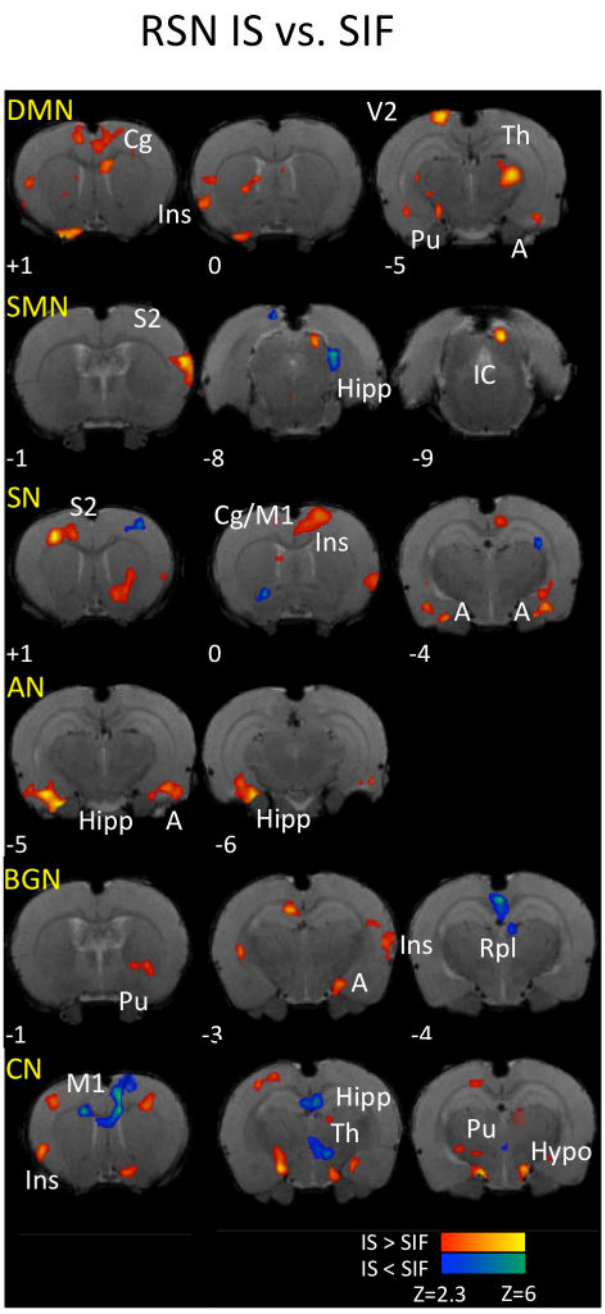

Figure 4. Changes in Brain Resting State Networks in IS rats

Comparing IS vs. SIF treated RSN resulted in mostly increased connectivity of brain networks with several brain structures. Key: DMN: Default Mode Network; SMN: Sensorimotor Network; SN: salience network; AN: Autonomic network; BGN: Basal ganglia networks; CN: Cerebellar network; Cg: cingulate cortex; Ins: insula; Pu: Caudate/Putamen; V2: Secondary Visual; Th: Thalamus; S2; secondary somatosensory; A: amygdala; Hipp: hippocampus; IC: inferior colliculus; M1: Primary Motor; Rpl: retrosplenial; Hypo: Hypothalamus. For specific subdivisions of some brain structures, please see text and Table 1.

TABLE 1

IS vs. SIF Changes in Evoked Mechanical Stimulation

Brain Structure	**Laterality**	**Zstat**	**X(mm)**	**Y(mm)**	**Z(mm)**	**Volume (mm3)**
Positive (IS > SIF) Cortical			(mm)	(mm)	(mm)	(mm3)
Primary Somatosensory Barrel Field	L	2.47	−3.87	8.55	−3.00	4.31
	R	2.18	3.98	8.32	−3.00	0.96
Dysgranular Region	R	2.51	3.05	7.62	−3.00	4.28
SubCortical						
Caudate Putamen	L	2.25	−3.87	3.28	0.00	1.18
Extended Amygdala Medial Division	R	2.37	0.82	2.81	−1.00	0.92
Hippocampal Formation CA1 Field	L	2.86	−1.76	7.15	−3.00	6.34
Hippocampal Formation CA3 Field	L	2.77	−5.51	3.16	−5.00	2.47
Thalamus (vpl/vpm)	L	2.71	−3.17	3.40	−4.00	12.25
Thalamus (vpl)	R	3.24	2.58	2.93	−4.00	2.76
Thalamus (vpm)	R	2.81	1.87	2.81	−4.00	1.98
Thalamus (vm)	R	2.73	0.47	2.58	−4.00	1.25
Thalamus (vm)	R	2.70	0.82	2.34	−4.00	2.10
Hypothalamus Medial Zone	L	2.37	−0.12	1.29	−4.00	1.80
Fimbria-Fronix	R	2.30	3.51	3.28	−5.00	1.19
Deep Mesencephalic nucelus	R	2.52	1.17	3.16	−6.00	1.74
Periaqueductal Gray Lateral Column Zone	R	2.20	0.35	4.45	−8.00	1.26
Reticular Formation Pontomedullary	L	2.87	0.00	1.05	−10.00	1.44
	L	2.72	−0.82	1.05	−10.00	1.92
Cranial Branchiometic Motor Nuclei	L	2.22	−2.93	1.87	−10.00	1.52
Cerebellum/Brainstem						
Simple Lobule	R	2.24	2.46	7.03	−11.00	2.80
Cerebellar Peduncle	R	2.49	2.69	3.05	−12.00	2.27
Cranial Somatic Senory Nuclei	R	2.92	1.76	2.93	−13.00	2.25
Medullary Relay Nuclei	R	2.72	0.94	3.40	−13.00	1.76
Ansiform Lobule Crus 2	R	2.68	3.16	7.27	−13.00	1.79
Paramedian Lobule	R	2.50	3.63	4.80	−13.00	1.96
Cerebellum Lobule 07	R	2.43	3.28	5.39	−13.00	1.50

Brain Structure	Laterality	Zstat	X(mm)	Y(mm)	Z(mm)	Volume (mm3)
Negative (IS < SIF) Cortical						
Retrosplenial Cortex	L	1.68	−1.17	7.73	−9.00	2.03

TABLE 2

IS vs. SIF Changes in Brain Networks

Default Mode Network Brain Structure	**Laterality**	**Zstat**	**X(mm)**	**Y(mm)**	**Z(mm)**	**Volume (mm3)**
Positive (IS>SIF) Cortical						
Insular Cortex	R	2.36	4.92	4.1	1	1.18
		2.29	5.04	2.81	0	2.5
Cingulate Cortex	L	2.04	−0.24	6.91	1	12.8
Motor Cortex Secondary	R	2.01	0.94	8.44	1	3.54
Somatosensory Cortex Primary Barrel Field	R	2.33	4.92	5.62	−1	3.14
		3.19	4.1	6.44	−2	1.3
	L	2.6	−5.04	6.44	−2	2.16
Somatosensory Cortex Secondary	L	2.48	−5.74	4.45	−2	2.24
Perirhinal Cortex	R	2.25	5.39	3.75	−8	2.55
	L	2.31	−6.21	3.28	−3	1.65
Visual Cortex Secondary	R	3.58	1.76	9.26	−5	2.06
		2.6	1.4	8.91	−7	2.68
	L	2.88	−5.86	6.44	−7	4.13
Subcortical						
Caudate Putamen	R	2.3	2.11	3.63	0	2.55
		2.01	3.4	4.1	0	1.17
Fimbria - Fronix	L	2.71	−1.88	6.09	−2	1.47
		2.47	−2.7	7.73	−4	1.57
Hypothalamus Medial Zone	L	3.35	−0.24	1.64	−3	1.21
Thalamus Posterior Nucleus	L	3.49	−3.4	4.8	−5	7.77
Amygdaloid Nuclear Complex Laterobasal	R	2.7	4.57	2.46	−4	1.13
	L	2.06	−5.39	1.64	−5	1.46
Hippocampal Formation CA2 Field	R	1.93	4.57	3.28	−6	1.43
Reticular Formation Pontomedullary	L	3.16	−1.53	1.99	−9	3.45
Negative (IS < SIF) Subcortical						
Cerebellum Lobule 08	L	3.02	−1.53	6.44	−13	1.26
Sensorimotor Network Brain Structure	**Laterality**	**Zstat**	**X(mm)**	**Y(mm)**	**Z(mm)**	**Volume (mm3)**
Positive (IS > SIF) Cortical						

Default Mode Network Brain Structure	**Laterality**	**Zstat**	**X(mm)**	**Y(mm)**	**Z(mm)**	**Volume (mm3)**
Somatosensory Cortex Secondary	L	3.47	−6.21	5.27	−1	3.38
Somatosensory Cortex Primary Upper Lip Region	L	3.34	−5.51	5.27	1	2.75
Subcortical						
Caudate Putamen	L	2.83	−4.34	2.46	0	1.04
Rubral Area	L	3.24	−0.24	2.46	−7	1.28
Inferior Colliculus	L	3.83	−1.88	6.91	−9	1.26
Negative (IS < SIF) Cortical						
Visual Cortex Secondary	R	3.23	1.4	8.55	−6	1.73
Subcortical						
Hippocampal Formation Subicular Complex	L	3.26	−3.4	5.62	−8	1.7
Salience Network Brain Structure	**Laterality**	**Zstat**	**X(mm)**	**Y(mm)**	**Z(mm)**	**Volume (mm3)**
Positive (IS > SIF) Cortical						
Somatosensory Cortex Primary Forelimb Region	R	4.29	2.93	6.56	1	2.02
Insular Cortex	L	1.92	−5.51	3.63	1	2.1
Motor Cortex Secondary	R	2.56	1.4	6.8	1	1.22
Motor Cortex Primary	L	2.76	−1.88	8.44	0	9.89
Somatosensory Cortex Primary Barrel Field	L	2.2	−3.75	7.73	−2	1.52
	L	2.92	−3.87	8.91	−3	1.07
Somatosensory Cortex Primary Trunk Region	L	2.9	−3.05	8.91	−3	1.54
Subcortical						
Caudate Putamen	L	2.39	−2.58	2.46	1	1.1
		2.36	−1.88	2.11	1	2.16
	L	2.16	−3.05	3.75	1	1.25
Hippocampal Formation CA3 Field	L	3.04	−4.57	2.11	−5	1.5
Hippocampal Formation CA2 Field	R	2.53	4.92	3.28	−6	1.29
Negative (IS<SIF) Cortical						
Somatosensory Cortex Primary Jaw Region	L	2.6	−3.87	7.62	1	1.19
Subcortical						
Fimbria - Fronix	L	2.82	−3.87	5.74	−3	1.06
		3.31	−4.34	7.27	−6	1.18
Reticular Formation Midbrian	R	3.11	2.22	3.28	−7	1.11

Default Mode Network Brain Structure	**Laterality**	**Zstat**	**X(mm)**	**Y(mm)**	**Z(mm)**	**Volume (mm3)**
Ansiform Lobule Crus 1	L	2.79	−5.04	5.74	−11	1.02
Autonomic Network Brain Structure	**Laterality**	**Zstat**	**X(mm)**	**Y(mm)**	**Z(mm)**	**Volume** (mm3)
Positive (IS > SIF)						
Subcortical						
Olfactory Amygdala	R	4.41	4.1	1.29	−5	2.43
Amygdaloid Nuclear Complex Laterobasal	L	3.4	−5.39	1.76	−5	2.4
Hippocampal Formation CA1 Field	R	3.95	2.93	1.29	−6	1.58
		3.35	3.75	2.11	−6	1.22
Basal Ganglia Brain Structures	**Laterality**	**Zstat**	**X(mm)**	**Y(mm)**	**Z(mm)**	**Volume (mm3)**
Positive (IS > SIF) Cortical						
Somatosensory Cortex Secondary	L	2.6	−5.86	6.44	−4	2.51
Insular Cortex	L	2.43	−6.33	4.45	−3	1.02
Visual Cortex Primary	L	3.17	−4.22	8.09	−7	1.76
Visual Cortex Secondary	R	2.83	3.75	6.09	−9	2.69
Temporal Association Cortex	R	2.26	4.22	4.92	−9	1.15
Subcortical						
Ventral Pallidum	R	2.85	2.11	1.29	1	1.91
Caudate Putamen	L	3.11	−3.87	2.81	−1	1.21
Extended Amygdala Medial Division	L	2.3	−2.7	1.64	−2	3.21
Negative (IS<SIF) Cortical						
Retrosplenial Cortex	L	3.52	−0.24	7.62	−4	2.33
Olfactory Cortex Lateral	R	2.89	4.92	1.29	−5	1.7
Subcortical	R					
Simple Lobule		3.56	2.93	6.09	−11	1.43
Cerebellum Network Brain Structure	**Laterality**	**Zstat**	**X(mm)**	**Y(mm)**	**Z(mm)**	**Volume (mm3)**
Positive (IS > SIF) Cortical						
Insular Cortex	R	2.78	4.92	2.93	1	1.44
Somatosensory Cortex Primary Jaw Region	R	2.33	4.1	6.8	1	1.17
Temporal Association Cortex	L	2.46	−5.51	6.09	−9	1.51
Subcortical						
Septal Region Medial Group	L	2.7	−0.24	1.64	0	1.17

Default Mode Network Brain Structure	Laterality	Zstat	X(mm)	Y(mm)	Z(mm)	Volume (mm3)
Extended Amygdala Medial Division	L	3.18	−1.76	3.28	−1	3.16
Hypothalamus Lateral Zone	R	3.39	2.11	1.29	−3	3.31
	L	3.01	−1.88	1.29	−4	1.88
Hippocampal Formation Dentate Gyrus	R	2.41	4.1	4.1	−7	1.4
Hippocampal Formation Subicular Complex	R	2.14	3.4	5.27	−8	1.41
Inferior Colliculus	L	2.93	−2.35	4.8	−9	1.79
Cerebellum Lobule 04	L	2.93	−0.24	7.27	−11	1.25
Negative (IS<SIF) Cortical						
Motor Cortex Primary	L	2.88	−1.88	7.73	1	1.22
Visual Cortex Secondary	R	3.21	4.57	6.91	−6	2.77
Subcortical						
Caudate Putamen	R	3.15	1.76	6.09	1	1.59
Hippocampal Formation CA3 Field	L	3.27	−0.59	6.09	−2	2.01
Thalamus Ventral Medial Nucleus	L	2.43	−1.06	2.81	−3	1.19
Ansiform Lobule Crus 1	L	3.16	−5.04	6.91	−11	1.69